

Journal of Materials Chemistry A

Accepted Manuscript



This is an *Accepted Manuscript*, which has been through the Royal Society of Chemistry peer review process and has been accepted for publication.

Accepted Manuscripts are published online shortly after acceptance, before technical editing, formatting and proof reading. Using this free service, authors can make their results available to the community, in citable form, before we publish the edited article. We will replace this *Accepted Manuscript* with the edited and formatted *Advance Article* as soon as it is available.

You can find more information about *Accepted Manuscripts* in the [Information for Authors](#).

Please note that technical editing may introduce minor changes to the text and/or graphics, which may alter content. The journal's standard [Terms & Conditions](#) and the [Ethical guidelines](#) still apply. In no event shall the Royal Society of Chemistry be held responsible for any errors or omissions in this *Accepted Manuscript* or any consequences arising from the use of any information it contains.

COMMUNICATION

A General and Simple Method to Synthesize Well-crystallized Nanostructured Vanadium Oxides for High Performance Li-ion Batteries

Cite this: DOI: 10.1039/x0xx00000x

Received 00th January 2012,
Accepted 00th January 2012

DOI: 10.1039/x0xx00000x

www.rsc.org/

Liye Li^{a,b}, Pengcheng Liu^{a,b}, Kongjun Zhu^{a*}, Jing Wang^a, Jinsong Liu^{a,b} and Jinhao Qiu^a

A remarkably simple and effective high-temperature mixing method under hydrothermal conditions was applied to synthesize well-crystallized V₃O₇•H₂O nanobelts, VO₂ (B) nanosheets and VO₂ (A) nanorods with good performance for Li-ion batteries. Especially, V₃O₇•H₂O exhibited excellent electrochemical performance. And, outstanding electrochemical properties were explained through analysis of crystal structures.

Electrochemical energy storage has become a critical technology for smart grid storage, electric vehicles (EVs), hybrid electric vehicles (HEVs), and portable electronic devices because of the growing worldwide energy crisis. Lithium-ion batteries (LIBs) are attractive energy storage devices because of their relatively high energy density, long cycle life, and good environment compatibility.¹⁻⁸ Among various possible electrode materials, layered crystal structure transition metal (TM) oxides have the huge potential as electrode materials for LIBs because the existed layered structure benefits the diffusion of Li-ions, thus results in free and easy insertion and extraction.^{9, 10} As the typical layered TM oxides, vanadium oxides have been extensively studied in the past decades, and considered to be the high-capacity cathode materials for next-generation LIBs.¹¹⁻¹³ Among them, VO₂ (B) is one of the most attractive cathode materials because of the double layers of V₄O₁₀ with tunnels for rapid Li-ion insertion/de-insertion in active materials. Through the heat treatment of vanadium oxide aerogels, Baudrin *et al.*¹⁴ synthesized nanostructured VO₂ (B) that exhibited as high as 500 mAh/g specific capacity of initial cycling. Mai *et al.*¹⁵ synthesized nanoscroll-buffered hybrid nanostructural VO₂ (B) cathodes with high rates and long cycling performances through the hydrothermal-driven splitting

and self-rolled method. Another polymorphic form of vanadium dioxide, VO₂ (A), exhibits a layered crystal structure similar to that of VO₂ (B), and is considered to be a new alternative cathode material for LIBs.^{16, 17} Dai *et al.*¹⁸ prepared VO₂ (A) nanowires with the highest initial capacity of 277.1 mAh/g. However, because the synthesis and growth conditions of VO₂ (A) are very severe, the corresponding reports on the electrochemical performance of VO₂ (A) are very limited. Recently, except VO₂ (A), another kind of vanadium oxide, V₃O₇•H₂O, has caught our more and more focus because it has a typical layered structure and larger interlayer spacing than V₂O₅.¹⁹ So, V₃O₇•H₂O will become another most promising cathode material for LIBs. Mjejri *et al.*²⁰ proved that V₃O₇•H₂O possessed electrochemical activity. Mohan *et al.*²¹ studied the cycling performance of V₃O₇•nH₂O. The initial capacity was 192 mAh/g, which decreased sharply to approximately 110 mAh/g after 40 cycles, which is possibly due to weak crystallinity and insufficient morphological control of products.

Although V₃O₇•H₂O, VO₂ (B), and VO₂ (A) are promising candidates as cathode materials for LIBs, their synthesis processes are comparatively complex, and synthesis methods are different and incompatible with each other, which will extremely increase the cost in industrial production because of the introduction of different production lines. Thus, an effective and simple method, by which different kinds of vanadium oxides with high crystallinity and performance can be obtained, is extremely essential for theoretical research, industrial production, and practical application. The high-temperature mixing method (HTMM), which is used under hydrothermal conditions, is a modified hydrothermal method.²²⁻²⁵ The starting solutions and raw materials for HTMM are separately heated to a desired reaction temperature in a double-chambered autoclave before mixing to initiate a hydrothermal reaction. The crystallinity of the obtained powders can be enhanced to improve the

properties of the final product. The results of our previous works revealed that HTMM will be an effective approach to synthesize vanadium oxides with high quality.²⁶

Herein, in this communication, the remarkably simple and effective high-temperature mixing method (HTMM) under hydrothermal conditions was applied to synthesize successfully three kinds of well-crystallized vanadium oxides, namely $V_3O_7 \cdot H_2O$ nanobelts, VO_2 (B) nanosheets and VO_2 (A) nanorods, with good performance for LIBs. Especially, $V_3O_7 \cdot H_2O$ exhibited excellent electrochemical performance. And, through the Rietveld refinement method, the crystal structures of vanadium oxides were analysed in detail to explain the outstanding electrochemical properties. Experimentally, the appropriate amount of V_2O_5 and oxalic acid were added respectively into two chambers of a Teflon-lined multi-chamber autoclave, and then these solutions were heated to the desired temperature and mixed for hydrothermal treatment for different time. The detailed experiment process was listed in Electronic Supplementary Information, ESI.

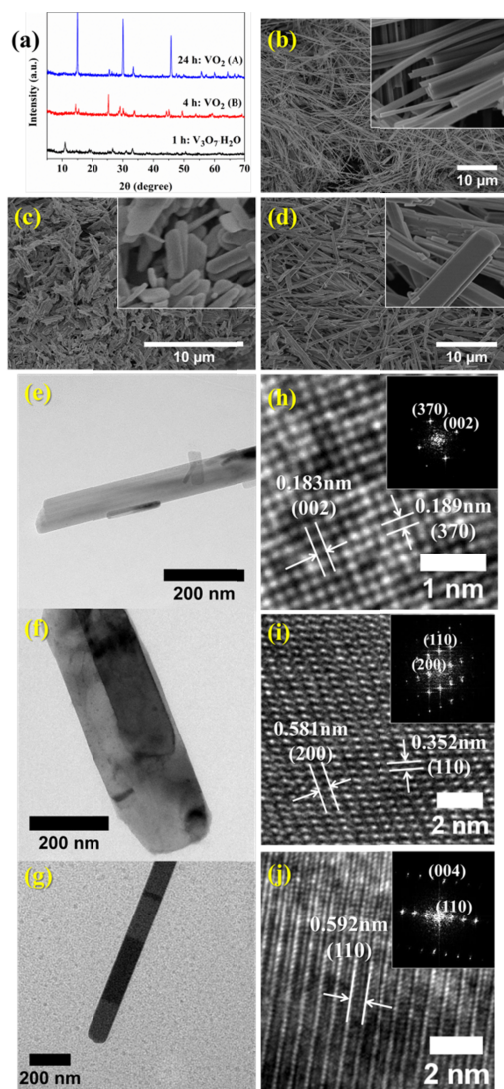


Fig. 1 Phase structure and morphology of products prepared by HTMM. (a) XRD patterns prepared for different time (standard JCPDS card No. 85-2401 for $V_3O_7 \cdot H_2O$, 81-2392 for VO_2 (B) and 70-2716 for VO_2 (A)); (b-d) SEM images of $V_3O_7 \cdot H_2O$, VO_2 (B) and VO_2 (A) respectively; (e-g) TEM images of $V_3O_7 \cdot H_2O$, VO_2 (B) and VO_2 (A) respectively; (h-j) HRTEM and SAED patterns of $V_3O_7 \cdot H_2O$, VO_2 (B) and VO_2 (A) respectively.

Figure 1 exhibits the phase structure and morphology of products prepared by HTMM. From Figure 1 (a), it can be seen that when the treatment time of hydrothermal reaction is 1 h, 4 h and 24 h, $V_3O_7 \cdot H_2O$, VO_2 (B) and VO_2 (A) can be obtained with high quality, respectively. Their interlayer spacing of some representative lattice planes has been calculated and listed in Table S1. Figures 1 (b) to (d) show the morphology characters of $V_3O_7 \cdot H_2O$ nanobelts, VO_2 (B) nanosheets and VO_2 (A) nanorods. The length change trend can be explained by the crystal growth mechanism of oriented attachment–exfoliation–recrystallization–oriented attachment. And, it has been described detailedly in our previous work.²⁶ Their morphology characters can be observed clearly further by TEM images [Figures 1 (e) to (g)]. Furthermore, the corresponding HRTEM images and fast Fourier transform (FFT) selected-area electron diffraction (SAED) patterns reveal further the high crystallinity of vanadium oxides prepared by HTMM [Figures 1 (h) to (j)]. The interlayer spacing observed agrees well with the calculate results of XRD. So, HTMM under hydrothermal conditions is a highly simple and general method for preparing nanostructured vanadium oxides with high qualities.

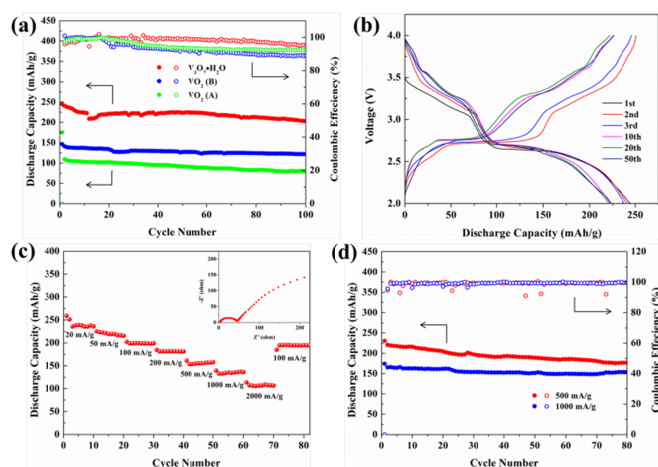
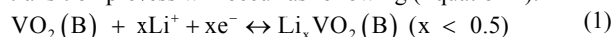


Fig. 2 Electrochemical measurements of $V_3O_7 \cdot H_2O$, VO_2 (B) and VO_2 (A). (a) Cycling properties at 100 mA/g of $V_3O_7 \cdot H_2O$ nanobelts, VO_2 (B) nanosheets and VO_2 (A) nanorods respectively; (b) charge-discharge curves of $V_3O_7 \cdot H_2O$ nanobelts at 100 mA/g; (c) rate properties of $V_3O_7 \cdot H_2O$ nanobelts; (d) cycling properties of high current density (500 and 1000 mA/g) for $V_3O_7 \cdot H_2O$ nanobelts.

Then, well-crystallized $V_3O_7 \cdot H_2O$ nanobelts, VO_2 (B) nanosheets and VO_2 (A) nanorods were assembled as the cathode of LIBs to investigate their electrochemical performance. Figure 2 (a) shows their discharge capacity during 100 cycles at 100 mA/g. It can be seen that three kinds of vanadium oxides exhibit good cycling performance. For VO_2 (B), the initial discharge capacity is 146.2 mAh/g, close to the theoretical capacity (161 mAh/g, $x=0.5$ in Li_xVO_2). After 100 cycles, 83% of its initial capacity can be kept. And, an obvious platform can be observed, when charged/discharged between 3.0 and 2.0 V as shown in Figure S1 (a). In this process, a phase transition process will occur as following (Equation 1):



The irreversible capacity lost in the first cycle is caused by the decomposition of electrolyte and the formation of solid electrolyte interface (SEI) layer.²⁷⁻²⁹ Figure S1 (b) shows its rate performance at progressively increased current density (ranging from 20 to 2000 mA/g). A discharge capacity of 90 mAh/g is obtained at 2000 mA/g (~22°C). When the current density is turned back to 100 mA/g, 98% of capacity can be recovered, and it is kept well in the following cycles. The performance of VO_2 (B) nanosheets is close to the

reports by Mai.¹⁵ But, it is worthy to be noticed that no surfactants, template agents and organic solvents were introduced in our HTMM synthesis. So, HTMM is more cost-save, green and effective. For VO₂ (A), the discharge capacity is 109.3 mAh/g in the initial cycle, and 79 mAh/g can be kept after 100 cycles. A discharge platform around 2.7 V is observed shown in Figure S2 (a). When the current is increased from 20 to 200 mA/g, the capacity decreases slightly, and a large capacity fade is observed when the current is increased further. But, after current density is turned back to 100 mA/g, 92% of capacity can be recovered.

Excitingly, for V₃O₇•H₂O nanobelts, its initial discharge capacity is up to 244.6 mAh/g, which realizes close to 90% theoretical capacity of 280 mAh/g. Then, it shows a trivial capacity decrease in the initial cycles, followed by a slow increase in the subsequent cycles up to 55 cycles before stabilizing. As for the discharge capacity increase in the cycling, it can be explained by the activation process that is caused by the gradual wetting by the electrolyte soaking, as well as a larger active surface caused by the nanosize effects that have been reported in previous works.^{30, 31} After 100 cycles, the capacity of 202 mAh/g can be kept, corresponding 83% of the initial capacity. It reveals that V₃O₇•H₂O nanobelts possess quite good cycling performance. Figure 2 (b) shows its charge-discharge patterns. After 10 cycles, the discharge and charge curve are well overlapped, which also indicates the high reversibility and good capacity retention of the electrode. And, multiple voltage plateaus mean the multi-step Li-ions intercalation and deintercalation process. To evaluate further the advantage of V₃O₇•H₂O nanobelts prepared by HTMM, rate performance at progressively increased current density ranging from 20 to 2000 mA/g were measured, as shown in Figure 2 (c). A discharge capacity of 114 mAh/g is obtained at 2000 mA/g (18 C). Even suffering from rapid charge-discharge of the current density, the electrode still shows stable capacity at each current. When the current density is turned back to 100 mA/g, 98% of capacity can be recovered, and there is no obvious capacity loss in the following cycles. The superior rate property of V₃O₇•H₂O is related to the low resistance of 50 Ω [inset of Figure 2 (c)] which is less obviously than of VO₂ (B) [inset of Figure S1 (b)] and VO₂ (A) [inset of Figure S2 (b)]. The cycling of V₃O₇•H₂O nanobelts cathode at high current density of 500 (2 C) and 1000 mA/g (6 C) is subsequently shown in Figure 2 (d). The initial discharge capacity of 230 and 172.9 mAh/g can be obtained respectively. And, the capacity retentions are 81% and 89% respectively after the following cycles. Meanwhile, the coulombic efficiency stays close to 100%. It should be noticed that the cycling performance seems better at large current density. This may be caused by two reasons. One is that the intercalation/deintercalation mechanism of Li-ions may show supercapacitor character during fast charge/discharge process, which will keep the capacity more stable at large current density.³² Another reason is that the dissolution character is common for vanadium oxide in cycling. The fast charge/discharge process can shorten the time when the active materials are soaked in electrolyte, so that the cycling will keep more stable at large current density.^{15, 33} Above results show that nanostructured vanadium oxides prepared by highly simple HTMM possess superior electrochemical performance.

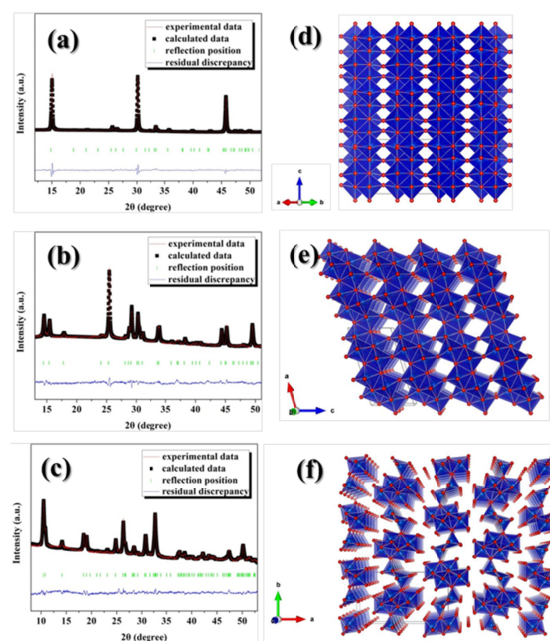


Fig. 3 Crystal structure analysis of V₃O₇•H₂O nanobelts, VO₂ (B) nanosheets and VO₂ (A) nanorods. (a-c) Rietveld refinement patterns of V₃O₇•H₂O, VO₂ (B) and VO₂ (A) respectively; (d-f) corresponding structure models of V₃O₇•H₂O, VO₂ (B) and VO₂ (A) respectively.

To investigate further the difference of electrochemical performances of V₃O₇•H₂O nanobelts, VO₂ (B) nanosheets and VO₂ (A) nanorods, the Rietveld refinement method was applied to analyze their crystal structures. Their XRD results were refined by Rietveld method (as implemented by the FullProf software suite) as shown in Figures 3 (a) to (c). The detailed data are listed in Table S2. Their corresponding structure models are also shown in Fig. 4(d-f) respectively. All of their crystal structures are established by the stacking of V-O layers. However, there are still some differences among them. For VO₂ (B) and VO₂ (A), through the stacking of V-O layers, abundant tunnels form, which function as pathways for the Li⁺ diffusion during insertion and extraction in their crystal structures.^{18, 34} And, it can be also observed clearly that the cross section of tunnels existed in VO₂ (B) is much bigger than ones of VO₂ (A). So, Li-ions can diffuse more easily in the crystal structure. It is also the reason why the capacity, cycling and rate performances of VO₂ (B) are better than VO₂ (A). However, for V₃O₇•H₂O, the pathway of Li-ions is different. The reason is that the V-O layers don't contact with each other because of the existence of crystal water molecules between interlayers that can be indexed through the H-O-H stretching vibration of 3451.59 cm⁻¹ in FTIR spectra²⁴ shown in Figure S3. So, the large interlayers are kept with the spacing of 0.807 nm, which agrees well with XRD results. Compared with the diffusion in tunnels, Li-ions will migrate more freely between interlayers,^{9, 10, 36} which is consistent well with the results of EIS measurement. So, V₃O₇•H₂O nanobelts cathodes exhibit excellent electrochemical performance.

Conclusions

In summary, the remarkably simple and effective high-temperature mixing method (HTMM) under hydrothermal conditions was applied to synthesize successfully three kinds of well-crystallized vanadium oxides, namely V₃O₇•H₂O nanobelts, VO₂ (B) nanosheets and VO₂ (A) nanorods, with good performance for LIBs. Especially, V₃O₇•H₂O exhibits superior electrochemical performance. And,

through the Rietveld refinement method, the crystal structures of vanadium oxides were analysed in detail to explain the differences of their electrochemical properties. Importantly, this method can be extended to synthesize other vanadium oxides for high performance LIBs.

Notes and references

†Liye Li and Pengcheng Liu contributed equally to this work.

^a State Key Laboratory of Mechanics and Control of Mechanical Structures, Nanjing University of Aeronautics and Astronautics, Nanjing 210016, China

^b College of Materials Science and Technology, Nanjing University of Aeronautics and Astronautics, Nanjing 210016, China

Electronic Supplementary Information (ESI) available: experiment section; interlayer spacing and detailed refinement results of $V_3O_7 \cdot H_2O$ nanobelts, VO_2 (B) nanosheets and VO_2 (A) nanorods; electrochemical performances of VO_2 (B) nanosheets and VO_2 (A) nanorods; FTIR patterns $V_3O_7 \cdot H_2O$ nanobelts. See DOI: 10.1039/c000000x/

* E-mail: kjzhu@nuaa.edu.cn

† This work was supported by the National Nature Science Foundation of China (NSFC No. 51172108), A Project Funded by the Priority Academic Program Development of Jiangsu Higher Education Institutions (PAPD), Qing Lan Project, Funding of Jiangsu Innovation Program for Graduate Education (NO. KYLX_0262), the Fundamental Research Funds for the Central Universities.

1. B. Dunn, H. Kamath and J.-M. Tarascon, *Science*, 2011, **334**, 928-935.
2. N. Liu, H. Wu, M. T. McDowell, Y. Yao, C. Wang and Y. Cui, *Nano letters*, 2012, **12**, 3315-3321.
3. J. B. Goodenough and Y. Kim, *Chemistry of Materials*, 2010, **22**, 587-603.
4. M. M. Thackeray, C. Wolverton and E. D. Isaacs, *Energy & Environmental Science*, 2012, **5**, 7854.
5. H. Ren, R. Yu, J. Wang, Q. Jin, M. Yang, D. Mao, D. Kisailus, H. Zhao and D. Wang, *Nano letters*, 2014, **14**, 6679-6684.
6. J. Wang, N. Yang, H. Tang, Z. Dong, Q. Jin, M. Yang, D. Kisailus, H. Zhao, Z. Tang and D. Wang, *Angewandte Chemie International Edition*, 2013, **52**, 6417-6420.
7. X. Lai, J. E. Halpert and D. Wang, *Energy & Environmental Science*, 2012, **5**, 5604-5618.
8. S. Xu, C. M. Hessel, H. Ren, R. Yu, Q. Jin, M. Yang, H. Zhao and D. Wang, *Energy & Environmental Science*, 2014, **7**, 632-637.
9. A. R. Armstrong and P. G. Bruce, *Nature*, 1996, **381**, 499-500.
10. M. H. Han, E. Gonzalo, G. Singh and T. Rojo, *Energy Environ. Sci.*, 2014, **8**, 81-102.
11. A. Pan, H. B. Wu, L. Yu and X. W. D. Lou, *Angewandte Chemie*, 2013, **125**, 2282-2286.
12. R. Cava, A. Santoro, D. Murphy, S. Zahurak, R. Fleming, P. Marsh and R. Roth, *Journal of solid state chemistry*, 1986, **65**, 63-71.
13. X.-F. Zhang, K.-X. Wang, X. Wei and J.-S. Chen, *Chemistry of Materials*, 2011, **23**, 5290-5292.
14. E. Baudrin, G. Sudant, D. Larcher, B. Dunn and J.-M. Tarascon, *Chemistry of materials*, 2006, **18**, 4369-4374.
15. L. Mai, Q. Wei, Q. An, X. Tian, Y. Zhao, X. Xu, L. Xu, L. Chang and Q. Zhang, *Advanced materials*, 2013, **25**, 2969-2973.
16. S. Ji, Y. Zhao, F. Zhang and P. Jin, *Journal Of the Ceramic Society Of Japan*, 2010, **118**, 867-871.
17. S. Ji, F. Zhang and P. Jin, *Journal Of Solid State Chemistry*, 2011, **184**, 2285-2292.
18. L. Dai, Y. Gao, C. Cao, Z. Chen, H. Luo, M. Kanehira, J. Jin and Y. Liu, *Rsc Advances*, 2012, **2**, 5265-5270.
19. A. M. Chippindale and P. G. Dickens, *J. Mater. Chem.*, 1992, **2**, 601-607.
20. I. Mjejri, N. Etteyeb and F. Sediri, *Materials Research Bulletin*, 2013, **48**, 3335-3341.
21. V. Mohan, K. Murakami and W. Chen, *Ionics*, 2012, **18**, 607-614.
22. H. Gu, K. Zhu, X. Pang, B. Shao, J. Qiu and H. Ji, *Ceramics International*, 2012, **38**, 1807-1813.
23. K. Zhu, K. Yanagisawa, R. Shimanouchi, A. Onda, K. Kajiyoshi and J. Qiu, *Materials Research Bulletin*, 2009, **44**, 1392-1396.
24. K. Zhu, K. Yanagisawa, A. Onda, K. Kajiyoshi and J. Qiu, *Materials Chemistry And Physics*, 2009, **113**, 239-243.
25. K. Zhu, Y. Cao, X. Wang, L. Bai, J. Qiu and H. Ji, *Crystengcomm*, 2012, **14**, 411-416.
26. P. Liu, K. Zhu, Y. Gao, Q. Wu, J. Liu, J. Qiu, Q. Gu and H. Zheng, *CrystEngComm*, 2013, **15**, 2753-2760.
27. D. Su, C. Wang, H. Ahn and G. Wang, *Physical Chemistry Chemical Physics*, 2013, **15**, 12543.
28. J.-Y. Shin, D. Samuelis and J. Maier, *Advanced Functional Materials*, 2011, **21**, 3464-3472.
29. J. S. Chen, Y. L. Tan, C. M. Li, Y. L. Cheah, D. Luan, S. Madhavi, F. Y. C. Boey, L. A. Archer and X. W. Lou, *Journal of the American Chemical Society*, 2010, **132**, 6124-6130.
30. K. Cao, L. Jiao, H. Liu, Y. Liu, Y. Wang, Z. Guo and H. Yuan, *Advanced Energy Materials*, 2015, **5**, n/a-n/a.
31. X. Huang, H. Yu, J. Chen, Z. Lu, R. Yazami and H. H. Hng, *Advanced materials*, 2014, **26**, 1296-1303.
32. D. Chao, C. Zhu, X. Xia, J. Liu, X. Zhang, J. Wang, P. Liang, J. Lin, H. Zhang, Z. X. Shen and H. J. Fan, *Nano letters*, 2014.
33. D. Chao, X. Xia, J. Liu, Z. Fan, C. F. Ng, J. Lin, H. Zhang, Z. X. Shen and H. J. Fan, *Advanced materials*, 2014, **26**, 5794-5800.
34. S. Zhang, Y. Li, C. Wu, F. Zheng and Y. Xie, *The Journal of Physical Chemistry C*, 2009, **113**, 15058-15067.
35. M. K. Chine, *Materials Sciences and Applications*, 2011, **02**, 964-970.
36. D. Aurbach, B. Markovsky, I. Weissman, E. Levi and Y. Ein-Eli, *Electrochimica acta*, 1999, **45**, 67-86.